Generalized Quantum Measurement in Spin-Correlated Hyperon-Antihyperon Decays

Sihao Wu(吴思浩)[1], Chen Qian(钱辰)[2*], Yang-Guang Yang(杨阳光)[3], and Qun Wang(王群)[1,4]

[1]*Department of Modern Physics, University of Science and Technology of China, Hefei 230026, China*
[2]*Beijing Academy of Quantum Information Sciences, Beijing 100193, China*
[3]*Institute of Modern Physics, Chinese Academy of Sciences, Lanzhou 730000, China*
[4]*School of Mechanics and Physics, Anhui University of Science and Technology, Huainan 232001, China*

(Received 26 July 2024; accepted manuscript online 25 September 2024)

The rapid developments of quantum information science (QIS) have opened up new avenues for exploring fundamental physics. Quantum nonlocality, a key aspect for distinguishing quantum information from classical one, has undergone extensive examinations in particles' decays through the violation of Bell-type inequalities. Despite these advancements, a comprehensive framework based on quantum information theory for particle interaction is still lacking. Trying to close this gap, we introduce a generalized quantum measurement description for decay processes of spin-1/2 hyperons. We validate this approach by aligning it with established theoretical calculations and apply it to the joint decay of $\Lambda\bar{\Lambda}$ pairs. We employ quantum simulation to observe the violation of Clauser–Horne–Shimony–Holt inequalities in $\eta_c/\chi_{c0} \to \Lambda\bar{\Lambda}$ processes. Our generalized measurement description is adaptable and can be extended to a variety of high energy processes, including decays of vector mesons, J/ψ, $\psi(2S) \to \Lambda\bar{\Lambda}$, in the Beijing Spectrometer III (BESIII) experiment at the Beijing Electron Positron Collider (BEPC). The methodology developed in this study can be applied to quantum correlation and information processing in fundamental interactions.

DOI: 10.1088/0256-307X/41/11/110301

1. Introduction. Quantum field theory based on quantum mechanics and special relativity is an underlying theory for elementary particles and their interactions. Quantum information theory can offer us a new perspective for research of elementary particles and their interactions.[1,2] An essential feature of quantum mechanics is quantum nonlocality characterized by the violation of Bell-type inequalities.[3–5] So far, these Bell-type inequalities have been widely applied in photonic and atomic systems detecting quantum correlation of electromagnetic interaction at low energy.[6,7] High-energy processes also provide an alternative testing ground for quantum nonlocality in electroweak and strong interactions[8,9] with increasingly precise data. Recently there have been a lot of works along this line in different particle systems, e.g., the hyperon-antihyperon system in charmonium decays at Beijing Electron Positron Collider (BEPC),[10–17] the Λ hyperon pairs in string fragmentation,[18] the top quark and anti-top quark ($t\bar{t}$) system produced at Large Hadron Collider (LHC),[1,19–22] the leptons pairs from e^+e^- annihilation or Higgs decay,[23,24] and correlated vector bosons and Higgs bosons in high energy processes.[25–28] It is worth mentioning that the quantum entanglement in string fragmentation in high energy processes such as electron–positron and electron–proton collisions can be studied using the spin correlation of the hyperon-antihyperon system,[18,29] in which a modified version of the Clauser–Horne–Shimony–Holt (CHSH) inequality for mixed states has been proposed and can be tested.[18] The spin correlation of the hyperon-antihyperon system has also been studied in heavy-ion collisions and can provide information on the vorticity structure of the strong interaction matter.[30,31]

However, there are still some difficulties in testing Bell-type inequalities in particle physics. One difficulty is that it is hard to overcome all loopholes especially in high energy interactions.[32] The other is that we would encounter different Bell-type inequalities in different particle decays because decay parameters vary for different particles, which seems to lack a general feature.[13–15] For these reasons, we need to search for a general framework to describe quantum properties in high energy processes with the help of quantum information theory. Recently the decay processes of particles have been characterized as quantum measurement processes[14,15] with particle interactions interpreted as quantum channels.[2] Moreover, quantum tomography has been employed to analyze quantum correlation in top-antitop quark pairs.[1,19,22] Despite these works, a general framework for particle interactions in the viewpoint of quantum information theory has yet to be established.

The purpose of this study is to explore a mapping between the generalized quantum measurement and the particle decay process. We will focus on decays of spin-1/2 hyperons, especially $\Lambda\bar{\Lambda}$ hyperon pair from decays of spin-0 charmonia η_c and χ_{c0}. We describe decay processes of spin-1/2 hyperons in the language of generalized quantum

*Corresponding author. Email: qianchen@baqis.ac.cn
© 2024 Chinese Physical Society and IOP Publishing Ltd

measurement and quantum channel. The generalized measurement in Bloch–Fano representation is introduced in the Supplementary Material. Then we apply the method to study the quantum correlation in $\Lambda\bar{\Lambda}$ from decays of η_c and χ_{c0}. Finally, we perform the quantum simulation to test the CHSH inequality in $\Lambda\bar{\Lambda}$ and their decay daughters on the quantum computing platform *Quafu*.

In this Letter, we briefly review the concept of the generalized quantum measurement and decay parameters of spin-1/2 hyperons in Section 2, and then describe decay processes of spin-1/2 hyperons in the framework of the generalized measurement and quantum channel in Sections 3 and 4, respectively. We perform the quantum simulation to test the CHSH inequality in Section 5. We have a discussion about the connection between the quantum measurement and particle reaction processes in Section 6. A summary of the main result and outlook is given in Section 7.

2. Preliminaries. Here, we briefly review some concepts in quantum measurement theory and hyperon decays, which will be used in the following sections.

2.1 Generalized Measurement and Quantum Channel. In Quantum Information Science (QIS), the measurement postulate is employed to describe the act of measurement on a quantum system.[33] According to this postulate, the measurement processes in quantum physics are subject to a collection of *measurement operators* $\{M_m\}$. These processes are defined as *generalized measurements*, distinguishing from the well-known *projective measurements* or *von Neumann measurements*, which have to be orthogonal. When we use the density operator ρ to describe a system being measured, the probability of obtaining a certain outcome m is given by

$$\mathcal{P}(m) = \mathrm{Tr}(M_m \rho M_m^\dagger), \tag{1}$$

where $\{\mathcal{P}(m)\}$ are probability distributions for all possible outcomes satisfying the non-negative condition $\mathcal{P}(m) \geq 0$ and the normalization condition $\sum_m \mathcal{P}(m) = 1$. These two conditions lead to constraints on $\{M_m\}$: the positive semidefiniteness: $M_m^\dagger M_m \geq 0$, and the completeness: $\sum_m M_m^\dagger M_m = \mathbb{1}$. Based on the measurement postulate in quantum mechanics, the initial state ρ instantaneously transforms after the measurement to the state ρ_m,

$$\rho \mapsto \rho_m = \frac{M_m \rho M_m^\dagger}{\mathcal{P}(m)}, \tag{2}$$

where the subscript of ρ_m corresponds to the outcome m. One can also define the *positive operator-valued measurement* (POVM)[33] through the generalized measurement as $F_m \equiv M_m^\dagger M_m$ with the probability $\mathcal{P}(m) = \mathrm{Tr}(F_m \rho)$ following Eq. (1). The POVM formalism has been used in some recent works in high energy physics.[28]

Nevertheless, sometimes we cannot accurately obtain measurement outcomes in real experiments. That is, if we lose the track of some measurement outcomes, the resulting quantum states will be described by an ensemble $\{\mathcal{P}(m), \rho_m\}$, which indicates that the post-measurement state ρ_m has the probability $\mathcal{P}(m)$. Then, the post-measurement state is

$$\begin{aligned}\sum_m \mathcal{P}(m)\rho_m &= \sum_m \mathrm{Tr}(M_m \rho M_m^\dagger) \frac{M_m \rho M_m^\dagger}{\mathrm{Tr}(M_m \rho M_m^\dagger)} \\ &= \sum_m M_m \rho M_m^\dagger,\end{aligned} \tag{3}$$

which can be taken as a quantum evolution generated by the measurement. This process is often characterized as a *quantum channel* $\rho \mapsto \mathcal{E}(\rho) \equiv \sum_m M_m \rho M_m^\dagger$, and the set of $\{M_m\}$ is called *Kraus operators*. In this study, the measurement operators play the role of Kraus operators.

2.2 Decay Width and Parameters. Hyperons such as Λ, Σ, and Ξ are heavier than protons and neutrons and contain one or more strange quarks. In this work, we focus on hyperon decays. A typical hyperon decay is to another spin-1/2 baryon B' accompanied by a spin-0 meson M denoted as $B \to B'M$. According to the effective Lagrangian, the decay matrix element reads[34]

$$\mathcal{A}_{B\to B'M} = G_\mathrm{F} m_M^2 \bar{u}_{B'}(C_1 - C_2\gamma_5)u_B, \tag{4}$$

where G_F is the Fermi constant, m_M is the meson mass, and C_1 and C_2 are parity-violating s-wave and parity-conserving p-wave decay amplitudes. The partial decay width is given by

$$\Gamma = \frac{G_\mathrm{F}^2 m_M^4 |\boldsymbol{q}|}{4\pi m_B}(m_{B'} + E_{B'})(|S|^2 + |P|^2), \tag{5}$$

where m_B and $m_{B'}$ are the masses of the mother and daughter baryons respectively, $\boldsymbol{q}$ and $E_{B'} = \sqrt{|\boldsymbol{q}|^2 + m_{B'}^2}$ are the momentum and the energy of the daughter baryon in the rest frame of the mother baryon respectively, and the s- and p-wave amplitudes in Eq. (5) are connected with C_1 and C_2 in Eq. (4) by $S = C_1$ and $P = |\boldsymbol{q}|C_2/(m_{B'} + E_{B'})$. These S and P amplitudes are Lorentz scalars, C_1 and C_2 depend on the parities of final meson and baryon. In the decay angular distribution, we introduce three real parameters[35]

$$\alpha = \frac{2\mathrm{Re}(S^*P)}{|S|^2 + |P|^2},\ \beta = \frac{2\mathrm{Im}(S^*P)}{|S|^2 + |P|^2},\ \gamma = \frac{|S|^2 - |P|^2}{|S|^2 + |P|^2}, \tag{6}$$

which satisfy $\alpha^2 + \beta^2 + \gamma^2 = 1$, so α, β and γ are all in the range $[-1, 1]$. Note that one can use another parameterization $\beta = \sqrt{1-\alpha^2}\sin\phi$ and $\gamma = \sqrt{1-\alpha^2}\cos\phi$ with $\phi \in (-\pi, \pi]$.

3. Decay of Spin-1/2 Hyperons. In this section, we present our description of hyperon decays based on the theory of generalized quantum measurement. We mainly focus on the angular distribution of the daughter particle (baryon) and its connection with the generalized measurement description.

Using the quantum information language, a spin-1/2 particle such as octet baryon (n, p, Λ, $\Sigma^{\pm,0}$, $\Xi^{-,0}$) can be referred to as a qubit. The density operator describing a spin-1/2 particle or a qubit can be put into the Bloch representation as

$$\rho = \frac{1}{2}(\mathbb{1} + \boldsymbol{\sigma}\cdot\boldsymbol{s}), \tag{7}$$

where $\boldsymbol{\sigma} = (\sigma_x, \sigma_y, \sigma_z)$ is the vector of three Pauli matrices, $\mathbb{1}$ denotes the 2×2 unity matrix, and the vector

$\boldsymbol{s}$ is called *Bloch vector* or polarization vector to describe the polarization of the qubit. The Bloch vector $\boldsymbol{s}$ can be obtained by $\boldsymbol{s} = \langle\boldsymbol{\sigma}\rangle = \mathrm{Tr}(\rho\boldsymbol{\sigma})$.

3.1 Angular Distribution of Daughter Particle. To study the angular distribution of the outgoing baryon, we can write $\Gamma_{B\to B'M}$ derived from Eq. (4) in the form of an angular integration

$$\Gamma \propto \int \sum_{i=\pm} |\chi^{i\dagger}_{B'}(S + P\boldsymbol{\sigma}\cdot\boldsymbol{n})\chi_B|^2 \, d\Omega, \tag{8}$$

where χ_B and $\chi_{B'}$ represent spinors of mother and daughter baryons respectively, and $\boldsymbol{n} \equiv \boldsymbol{q}/|\boldsymbol{q}|$ represents the momentum direction of B'. The summation indicates a sum over the daughter baryon's spin state. We can rewrite Eq. (8) in a new form as

$$\frac{1}{\Gamma}\frac{d\Gamma}{d\Omega} = \mathrm{Tr}(M_{\boldsymbol{n}}\rho_B M^\dagger_{\boldsymbol{n}}), \tag{9}$$

where ρ_B denotes the spin density matrix for the mother baryon B, $d\Omega = d\boldsymbol{n} = d\cos\theta d\phi$, and the operator $M_{\boldsymbol{n}}$ is defined as

$$M_{\boldsymbol{n}} \equiv \frac{1}{\sqrt{4\pi(|S|^2 + |P|^2)}}(S + P\boldsymbol{\sigma}\cdot\boldsymbol{n}). \tag{10}$$

We can see from Eq. (9) that the determination of the angular distribution implies a generalized measurement characterized by the measurement operator $M_{\boldsymbol{n}}$. In this way, the particle decay can be regarded as a kind of generalized measurement process. The only difference here is that the discrete measurement outcome m described in Section 2 to a continuous direction $\boldsymbol{n}$ for the outgoing daughter baryon in experiments. It is necessary to validate the positive semidefiniteness and completeness of $\{M_{\boldsymbol{n}}\}$ as

$$M^\dagger_{\boldsymbol{n}} M_{\boldsymbol{n}} = \frac{1}{4\pi}(\mathbb{1} + \alpha\boldsymbol{\sigma}\cdot\boldsymbol{n}) \geq 0, \quad \text{for} \quad |\alpha| \leq 1,$$

and

$$\int M^\dagger_{\boldsymbol{n}} M_{\boldsymbol{n}} \, d\Omega = \mathbb{1}. \tag{11}$$

These two criteria ensure that $\{M_{\boldsymbol{n}}\}$ are legitimate measurement operators in QIS.

After defining the measurement operators, we proceed to calculate the decay process in this approach. According to the quantum measurement postulate, the probability for the momentum direction of the daughter baryon along $\boldsymbol{n}$ is given by $\mathcal{P}(\boldsymbol{n}) = \mathrm{Tr}(M_{\boldsymbol{n}}\rho_B M^\dagger_{\boldsymbol{n}})$, which exactly equals $(1/\Gamma)d\Gamma/d\Omega$ in Eq. (9). Given the initial spin density operator

$$\rho_B = \frac{1}{2}(\mathbb{1} + \boldsymbol{\sigma}\cdot\boldsymbol{s}_B), \tag{12}$$

as in Eq. (7), the resulting probability or the angular distribution reads

$$\begin{aligned}\mathcal{P}(\boldsymbol{n}) &= \mathrm{Tr}(M_{\boldsymbol{n}}\rho_B M^\dagger_{\boldsymbol{n}}) = \frac{1}{\Gamma}\frac{d\Gamma_{B\to B'M}}{d\Omega} \\ &= \frac{1}{4\pi}(1 + \alpha\boldsymbol{s}_B\cdot\boldsymbol{n}),\end{aligned} \tag{13}$$

which was first derived in Ref. [36].

Now we look at the polarization of the daughter baryon. According to the quantum measurement postulate, the spin density operator of the daughter baryon can be obtained via the post-measurement state in Eq. (2) as

$$\rho_{B'}(\boldsymbol{n}) = \frac{M_{\boldsymbol{n}}\rho_B M^\dagger_{\boldsymbol{n}}}{\mathrm{Tr}(M_{\boldsymbol{n}}\rho_B M^\dagger_{\boldsymbol{n}})} = \frac{1}{2}(\mathbb{1} + \boldsymbol{\sigma}\cdot\boldsymbol{s}_{B'}), \tag{14}$$

where $\boldsymbol{s}_{B'}$ is the polarization vector of the daughter baryon in the mother baryon's rest frame as a function of $\boldsymbol{n}$. By substituting ρ_B in Eq. (12) and $M_{\boldsymbol{n}}$ in Eq. (10) into Eq. (14), we obtain

$$\boldsymbol{s}_{B'} = \frac{(\alpha + \boldsymbol{s}_B\cdot\boldsymbol{n})\boldsymbol{n} + \beta(\boldsymbol{s}_B\times\boldsymbol{n}) + \gamma\boldsymbol{n}\times(\boldsymbol{s}_B\times\boldsymbol{n})}{1 + \alpha\boldsymbol{s}_B\cdot\boldsymbol{n}}, \tag{15}$$

where parameters α, β and γ are defined in Eq. (6). The explicit expression of $\boldsymbol{s}_{B'}$ in Eq. (15) was initially derived by Lee and Yang,[35] but here we rederived it in the language of generalized quantum measurement.

We can look at the decay process as a quantum channel induced by $\{M_{\boldsymbol{n}}\}$. In the hyperon decay process, the daughter baryon may fly in any direction $\boldsymbol{n}$ associated with the probability $\mathcal{P}(\boldsymbol{n})$, which is just the angular distribution of the daughter baryon in Eq. (13) that can be detected in particle physics experiments. With the daughter's spin density operator $\rho_{B'}(\boldsymbol{n})$, we have an ensemble $\{\mathcal{P}(\boldsymbol{n}), \rho_{B'}(\boldsymbol{n})\}$. According to the generalized measurement postulate in Eq. (3), this post-measurement ensemble can be interpreted as a quantum evolution in the channel $\mathcal{E}$ defined as

$$\mathcal{E}(\rho_B) = \int d\Omega \, M_{\boldsymbol{n}}\rho_B M^\dagger_{\boldsymbol{n}} = \frac{1}{2}\Big(\mathbb{1} + \frac{1+2\gamma}{3}\boldsymbol{\sigma}\cdot\boldsymbol{s}_B\Big). \tag{16}$$

Equation (16) is obtained via integrating Eqs. (14) and (15) and it is actually the ensemble average of the daughter baryon's spin density operator $\overline{\rho}_{B'} = \mathcal{E}(\rho_B)$, and the term $(1 + 2\gamma)\boldsymbol{s}_B/3$ represents the average polarization of the daughter baryon in the rest frame of the mother hyperon.

In summary, we have established in this subsection the quantum measurement interpretation for the nonleptonic decay of spin-1/2 hyperons. In the next subsection, we will introduce an alternative representation for the decay process.

3.2 Decay Chains. It is common for the daughter baryon to undergo subsequent decay, for example, in the decay chain $B \to B_1M_1 \to B_2M_2M_1$, in which B_1 decays to B_2M_2. This cascading decay process can be described by *the concatenate quantum measurement*. Then the joint angular distribution or joint probability is given by

$$\begin{aligned}\mathcal{P}(\boldsymbol{n}_1, \boldsymbol{n}_2) &= \frac{1}{\Gamma}\frac{d\Gamma}{d\Omega_1 d\Omega_2} \\ &= \mathrm{Tr}[M^{1\to2}_{\boldsymbol{n}_2} M^{B\to1}_{\boldsymbol{n}_1}\rho_B M^{\dagger B\to1}_{\boldsymbol{n}_1} M^{\dagger 1\to2}_{\boldsymbol{n}_2}],\end{aligned} \tag{17}$$

which is the probability that B_1 moving in the direction $\boldsymbol{n}_1$ decays to B_3 moving in the direction $\boldsymbol{n}_2$. Here $\{M^{B\to1}_{\boldsymbol{n}_1}\}$ and $\{M^{1\to2}_{\boldsymbol{n}_2}\}$ are two sets of measurement operators characterizing two decays, $B \to B_1M_1$ and $B_1 \to B_2M_2$, respectively.

4. Joint Decay of $B\bar{B}$ and Two-Qubit Correlations. In this section, we give a generalized quantum measurement

introduced in Section 3 for the joint decay of $B\bar{B}$ to $B'\bar{B}'$ and study the correlation between $B\bar{B}$ and $B'\bar{B}'$.

If we only consider the spin degree of freedom for two spin-1/2 particles, their joint state can be written in a general form

$$\rho_{B\bar{B}} = \frac{1}{4}\Big(\mathbb{1}_4 + \boldsymbol{s}_B\cdot\boldsymbol{\sigma}\otimes\mathbb{1}_2 + \mathbb{1}_2\otimes\boldsymbol{s}_{\bar{B}}\cdot\boldsymbol{\sigma} + \sum_{i,j} C_{ij}\sigma_i\otimes\sigma_j\Big), \tag{18}$$

where $i, j = 1, 2, 3$; $\mathbb{1}_n$ is the $n\times n$ unity matrix; $\boldsymbol{s}_B$ and $\boldsymbol{s}_{\bar{B}}$ are spin polarization vectors for B and $\bar{B}$, respectively; and C_{ij} is a 3×3 real matrix for the spin correlation between B and $\bar{B}$. Thus, there are 15 real parameters in $\rho_{B\bar{B}}$ corresponding to $s_B^i = \langle\sigma_i\otimes\mathbb{1}_2\rangle$, $s_{\bar{B}}^i = \langle\mathbb{1}_2\otimes\sigma_i\rangle$ and $C_{ij} = \langle\sigma_i\otimes\sigma_j\rangle$. The Hilbert spaces associated with spin states of B and $\bar{B}$ are denoted as $\mathscr{H}_B$ and $\mathscr{H}_{\bar{B}}$ respectively, thus $\rho_{B\bar{B}}$ describes a quantum state in the joint Hilbert space $\mathscr{H}_B\otimes\mathscr{H}_{\bar{B}}$. The one particle density operator can be obtained by taking the partial trace $\rho_B = \mathrm{Tr}_{\bar{B}}(\rho_{B\bar{B}}) = \frac{1}{2}(\mathbb{1}+\boldsymbol{s}_B\cdot\boldsymbol{\sigma})$ and $\rho_{\bar{B}} = \mathrm{Tr}_B(\rho_{B\bar{B}}) = \frac{1}{2}(\mathbb{1}+\boldsymbol{s}_{\bar{B}}\cdot\boldsymbol{\sigma})$, which reduces to Eq. (7) for one qubit.

4.1 Joint Decay of Baryon-Antibaryon with Spin Correlation. We consider the joint decay $B\bar{B}\to B'M\bar{B}'\bar{M}$ with spin correlation. According to the quantum measurement postulate, a joint decay process can be regarded as *parallel quantum measurement*. Then, the joint probability for this parallel measurement is given by

$$\mathcal{P}(\boldsymbol{n},\bar{\boldsymbol{n}}) = \mathrm{Tr}[(M_{\boldsymbol{n}}\otimes\bar{M}_{\bar{\boldsymbol{n}}})\rho_{B\bar{B}}\Big(M_{\boldsymbol{n}}^\dagger\otimes\bar{M}_{\bar{\boldsymbol{n}}}^\dagger\Big)], \tag{19}$$

similar to Eq. (14), where $\boldsymbol{n}$ or $\bar{\boldsymbol{n}}$ are momentum directions of B' and $\bar{B}'$ respectively, and $\{M_{\boldsymbol{n}}\}$ as well as $\{\bar{M}_{\bar{\boldsymbol{n}}}\}$ are measurement operators acting on $\mathscr{H}_B$ and $\mathscr{H}_{\bar{B}}$ respectively. In comparison with Eq. (13), the joint probability is actually the joint angular distribution of the daughter baryon and antibaryon. By substituting $M_{\boldsymbol{n}}$ and $\bar{M}_{\bar{\boldsymbol{n}}}$ in the form of Eq. (10) together with $\rho_{B\bar{B}}$ from Eq. (18) into Eq. (19), the joint angular distribution is given as

$$\frac{1}{\Gamma}\frac{d\Gamma(B\bar{B}\to B'M\bar{B}'\bar{M})}{d\Omega_{\boldsymbol{n}}d\Omega_{\bar{\boldsymbol{n}}}} = \frac{1}{(4\pi)^2}\Big[1+\alpha_B\boldsymbol{s}_B\cdot\boldsymbol{n}+\alpha_{\bar{B}}\boldsymbol{s}_{\bar{B}}\cdot\bar{\boldsymbol{n}}+\alpha_B\alpha_{\bar{B}}\sum_{i,j}C_{ij}n_i\bar{n}_j\Big], \tag{20}$$

where α_B and $\alpha_{\bar{B}}$ are decay parameters defined in Eq. (6) associated with B and $\bar{B}$ respectively.

The similar results can be found in Refs. [20,37] in the study of the correlated $t\bar{t}$ decay. T, an e joint angular distribution in Eq. (20) is derived in the generalized measurement approach. We note that the distribution in Eq. (19) is different from the one in Eq. (17), because the former describes the joint decay of $B\bar{B}$, while the latter describes the decay chain of B.

4.2 State Tomography and Experiments. In past decades, researchers intended to investigate quantum correlations in terms of Bell nonlocality in $\Lambda\bar{\Lambda}$ system produced by charmonium decays $(c\bar{c})\to\Lambda\bar{\Lambda}$. Some previous works proposed modified Bell-type inequalities[11–13] for the experimental test. The methods in these works rely heavily on elaborate modifications of Bell inequality and selected observables, which are hard to be implemented in experiments. There is no investigation into the two-qubit spin density operation of $\Lambda\bar{\Lambda}$ which is more powerful and efficient in the quantum correlation study. Recently a new method has been proposed and does not rely on any specific Bell-type inequality test in $t\bar{t}$ system[21,22] but makes use of the density operator of $t\bar{t}$. The method can be easily applied to the $\Lambda\bar{\Lambda}$ system.

Since the information of a system is fully encoded in the density operator, one can explore quantum properties through it. Therefore, in order to study the quantum correlation in the $\Lambda\bar{\Lambda}$ system, the key point is to determine the density operator $\rho_{\Lambda\bar{\Lambda}}$ in Eq. (18). In this subsection, we introduce how to obtain the two-qubit density matrix $\rho_{\Lambda\bar{\Lambda}}$ through the joint angular distribution in subsequent decays and its connection with generalized quantum measurement.

In the subsequent decay $\Lambda\bar{\Lambda}\to p(\pi^-)\bar{p}(\pi^+)$, the very direct observable is the joint angular distribution of the daughter proton p and antiproton $\bar{p}$:

$$\mathcal{P}(\theta,\bar{\theta}) = \frac{1}{(4\pi)^2}\Big[1+\alpha_\Lambda\sum_i s_i^\Lambda\cos\theta_i+\alpha_{\bar{\Lambda}}\sum_j s_j^{\bar{\Lambda}}\cos\bar{\theta}_j + \alpha_\Lambda\alpha_{\bar{\Lambda}}\sum_{i,j}C_{ij}\cos\theta_i\cos\bar{\theta}_j\Big], \tag{21}$$

where $\cos\theta_i = \boldsymbol{n}_i$ ($\cos\bar{\theta}_j = \bar{\boldsymbol{n}}_i$) for p ($\bar{p}$) with $\boldsymbol{n}$ ($\bar{\boldsymbol{n}}$) being the momentum direction of p ($\bar{p}$) in the rest frame of Λ ($\bar{\Lambda}$). Equation (21) is a reformulation of Eq. (20). By integration over $\bar{\theta}$, the marginal distribution of the proton is

$$\mathcal{P}(\theta) = \int d\bar{\Omega}\,\mathcal{P}(\theta,\bar{\theta}) = \frac{1}{4\pi}(1+\alpha_\Lambda\sum_i s_i^\Lambda\cos\theta_i), \tag{22}$$

which is a reformulation of Eq. (13).

The method of moments are widely used in experiments for the measurement of parameters. Obviously the first moment of $\cos\theta_i$ gives the polarization vector $\boldsymbol{s}_\Lambda$ as

$$\langle\cos\theta_i\rangle = \int d\Omega\,\mathcal{P}(\theta)\cos\theta_i = \frac{\alpha_\Lambda}{3}s_i^\Lambda. \tag{23}$$

A similar expression holds for $\cos\bar{\theta}_j$. As a consequence, the polarization of $\Lambda/\bar{\Lambda}$ can be measured by the arithmetic mean of $\cos\theta_i$ and $\cos\bar{\theta}_j$ in a sample of N events,

$$s_i^\Lambda = \frac{3}{\alpha_\Lambda}\langle\cos\theta_i\rangle = \frac{3}{\alpha_\Lambda}\frac{1}{N}\sum_{k=1}^N[\cos\theta_i]_{(k)},$$
$$s_j^{\bar{\Lambda}} = \frac{3}{\alpha_{\bar{\Lambda}}}\langle\cos\bar{\theta}_j\rangle = \frac{3}{\alpha_{\bar{\Lambda}}}\frac{1}{N}\sum_{k=1}^N[\cos\bar{\theta}_j]_{(k)}. \tag{24}$$

Similar to the polarization vector, the moment of $\cos\theta_i\cos\bar{\theta}_j$ gives the spin correlation matrix C_{ij} as

$$\langle\cos\theta_i\cos\bar{\theta}_j\rangle = \int d\Omega d\bar{\Omega}\,\mathcal{P}(\theta,\bar{\theta})\cos\theta_i\cos\bar{\theta}_j = \frac{\alpha_\Lambda\alpha_{\bar{\Lambda}}}{9}C_{ij}. \tag{25}$$

Consequently, C_{ij} can be measured in a sample of N events as

$$C_{ij} = \frac{9}{\alpha_\Lambda \alpha_{\bar\Lambda}} \langle \cos\theta_i \cos\bar\theta_j \rangle = \frac{9}{\alpha_\Lambda \alpha_{\bar\Lambda}} \frac{1}{N} \sum_{k=1}^{N} [\cos\theta_i \cos\bar\theta_j]_{(k)}. \tag{26}$$

With Eqs. (24) and (26), the two-qubit spin density operator $\rho_{\Lambda\bar\Lambda}$ in Eq. (18) is fully reconstructed. We express the $\rho_{\Lambda\bar\Lambda}$ in a compact form of $\rho_{\Lambda\bar\Lambda} = (1/4)\sum_{\mu,\nu} \Theta_{\mu\nu}\sigma_\mu \otimes \sigma_\nu$, with $\Theta_{00} = 1$, $\Theta_{i0} = s_i^\Lambda$, $\Theta_{j0} = s_j^{\bar\Lambda}$ and $\Theta_{ij} = C_{ij}$. The 4×4 matrix $\Theta_{\mu\nu}$ can be expressed as

$$\left[\begin{array}{c|c} 1 & \boldsymbol{s}_{\bar\Lambda}^{\mathrm{T}} \\ \hline \boldsymbol{s}_\Lambda & C_{ij} \end{array}\right] \Leftarrow \left[\begin{array}{c|c} \langle 1\rangle & \frac{3}{\alpha_{\bar\Lambda}}\langle \cos\bar\theta_j\rangle \\ \hline \frac{3}{\alpha_\Lambda}\langle \cos\theta_i\rangle & \frac{9}{\alpha_\Lambda\alpha_{\bar\Lambda}}\langle \cos\theta_i\cos\bar\theta_j\rangle \end{array}\right]. \tag{27}$$

The left-hand side of Eq. (27) has 15 real parameters which uniquely determine the two-qubit density operator $\rho_{\Lambda\bar\Lambda}$, while the right-hand side represents 15 moments from the data sample. The process of reconstructing the spin density matrix from experimental data is called *quantum state tomography*.[22,28] The generalized measurement formalism here serves as a bridge connecting the angular distribution of decay daughters to the spin density operator $\rho_{\Lambda\bar\Lambda}$.

With the spin density operator $\rho_{\Lambda\bar\Lambda}$, the Bell nonlocality can be measured by Horodecki observable as $\langle \mathcal{B}_{\mathrm{CHSH}}\rangle_{\max} = 2\sqrt{m_1 + m_2}$, with m_1 and m_2 being two largest eigenvalues of $C^{\mathrm{T}}C$.[38] The classical theory claims $\langle \mathcal{B}_{\mathrm{CHSH}}\rangle_{\max} \leq 2$, while the quantum theory claims $\langle \mathcal{B}_{\mathrm{CHSH}}\rangle_{\max} \leq 2\sqrt{2}$. The states having $\langle \mathcal{B}_{\mathrm{CHSH}}\rangle_{\max} > 2$ are said to be Bell nonlocal. So a measure for the Bell nonlocality can be defined as $\mathfrak{m}_{12}[\rho_{\Lambda\bar\Lambda}] = m_1 + m_2$ from the spin density operator.[21,24]

Now we look at the decay process $\eta_c/\chi_{c0} \to \Lambda\bar\Lambda$ and demonstrate the role of state tomography in studying the quantum correlation in the $\Lambda\bar\Lambda$ system.

According to quantum field theory, the joint angular distribution of $\eta_c/\chi_{c0} \to \Lambda\bar\Lambda \to p(\pi^-)\bar p(\pi^+)$ reads[12,13]

$$\begin{aligned} \frac{1}{\Gamma_{\eta_c}}\frac{d\Gamma_{\eta_c}}{d\Omega d\bar\Omega} &= \frac{1}{(4\pi)^2}(1 - \alpha_\Lambda\alpha_{\bar\Lambda}\boldsymbol{n}\cdot\bar{\boldsymbol{n}}), \\ \frac{1}{\Gamma_{\chi_{c0}}}\frac{d\Gamma_{\chi_{c0}}}{d\Omega d\bar\Omega} &= \frac{1}{(4\pi)^2}[1 + \alpha_\Lambda\alpha_{\bar\Lambda}(n_x\bar n_x + n_y\bar n_y - n_z\bar n_z)]. \end{aligned} \tag{28}$$

By comparing Eq. (28) with Eq. (21), the coefficients of $\rho_{\Lambda\bar\Lambda}$ are $\Theta_{\mu\nu} = \mathrm{diag}\{1, -1, -1, -1\}$ and $\Theta_{\mu\nu} = \mathrm{diag}\{1, 1, 1, -1\}$ in η_c and χ_{c0} decays, respectively. This confirms that η_c and χ_{c0} are in the spin singlet and triplet state of $c\bar c$ respectively.

In experiments, one can use the data to fit the joint angular distribution in Eq. (28), and thus reconstruct $\rho_{\Lambda\bar\Lambda}$ in Eq. (27). The measure of Bell nonlocality is a function of moments that are measured in experiments,

$$\mathfrak{m}_{12}[\rho_{\Lambda\bar\Lambda}] = \left(\frac{9}{\alpha_\Lambda\alpha_{\bar\Lambda}}\right)^2 [\langle \cos\theta_i\cos\bar\theta_i\rangle^2 + \langle \cos\theta_j\cos\bar\theta_j\rangle^2], \tag{29}$$

where $i, j = 1, 2, 3$ or x, y, z, and $i \neq j$. The above formula provides an easy test of nonlocality in experiments.

The quantum tomography offers a new approach to quantum correlations in high energy processes. In the quantum tomography approach, the measurement of probabilities can be replaced by that of the spin density matrix through kinematics of decay products in the $\Lambda\bar\Lambda$ system. However, we note that there is a loophole in Eq. (29), because $\alpha_\Lambda\alpha_{\bar\Lambda}$ are calculated from the framework of quantum mechanics. To solve this, we can consider Clauser–Horne (CH) inequality for future experiments as it has the form of probability. We have predicted a violation of CH inequality in Λ decays, which can be experimentally observed.[14]

In summary, the quantum tomography in terms of the spin density operator in Eq. (27) gives all information of the quantum state in a system, such as quantum nonlocality, quantum entanglement and/or quantum discord.[20] The method can be applied not only to spinless charmonium decays, but also to other high energy processes such as $e^-e^+ \to J/\psi, \psi(2S) \to \Lambda\bar\Lambda$. One can reconstruct the spin density operator from data and then decode quantum properties out of it.

5. Quantum Simulation. In this section, we perform quantum simulation for the decay of hyperon-antihyperon and present the test of the CHSH inequality through the spin correlation in the hyperon-antihyperon system.

5.1 Simulation for Generalized Measurement Process. Similar to $M_{\boldsymbol{n}}$ for the hyperon decay in Eq. (10), $\bar M_{\boldsymbol{n}}$ for the antihyperon decay is defined as

$$\bar M_{\boldsymbol{n}} = \frac{1}{\sqrt{4\pi}}\frac{1}{\sqrt{|\bar S|^2 + |\bar P|^2}}(\bar S + \bar P\boldsymbol{\sigma}\cdot\boldsymbol{n}), \tag{30}$$

which can be obtained from Eq. (10) by simply making the replacement $S \to \bar S$ and $P \to \bar P$.

In order to perform the simulation on the digital quantum computer, the measurement operators $\{M_{\boldsymbol{n}}\}$ must be embedded into unitary operators. It can be verified that the block matrix

$$U_{\boldsymbol{n}} \equiv \frac{1}{\sqrt{2(|S|^2 + |P|^2)}}\left[\begin{array}{c|c} S + P\boldsymbol{\sigma}\cdot\boldsymbol{n} & P^* - S^*\boldsymbol{\sigma}\cdot\boldsymbol{n} \\ \hline S - P\boldsymbol{\sigma}\cdot\boldsymbol{n} & P^* + S^*\boldsymbol{\sigma}\cdot\boldsymbol{n} \end{array}\right] \tag{31}$$

is unitary, and $M_{\boldsymbol{n}}$ is embedded as the upper-left block. From the definition of $M_{\boldsymbol{n}}$ in Eq. (10), it can be expressed by $M_{\boldsymbol{n}} = U(\mathcal{R})M_{\hat{\boldsymbol{z}}}U(\mathcal{R})^\dagger$, where $U(\mathcal{R})$ denotes an $SU(2)$ rotation isomorphic to $\mathcal{R}(\phi, \theta, 0)$. As a consequence, the unitary operator $U_{\boldsymbol{n}}$ can be obtained by performing a similarity transformation on $U_{\hat{\boldsymbol{z}}}$, as $U_{\boldsymbol{n}} = [\mathbb{1}\otimes U(\mathcal{R})]U_{\hat{\boldsymbol{z}}}[\mathbb{1}\otimes U(\mathcal{R})^\dagger]$. Similarly the unitary operator $\bar U_{\boldsymbol{n}}$ for the antihyperon decay can also be defined by the replacement $S \to \bar S$ and $P \to \bar P$.

Following this, the quantum circuit for simulating the joint decay of $\Lambda\bar\Lambda \to p\pi^-\bar p\pi^+$ is presented in Fig. 1, where the spin states of $\Lambda\bar\Lambda$ are prepared to be in the Bell states $|\Psi^\pm\rangle$ resulted from η_c/χ_{c0} decay as discussed in Section 4. Figure 1 indicates that the measurement operators have been successfully embedded into unitary operators, and the quantum information contained in $\Lambda\bar\Lambda$ can be extracted from ancilla qubits.

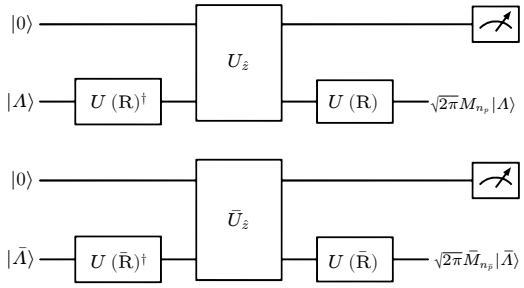

Fig. 1. The quantum circuit for generalized measurements. The spin states of Λ and $\bar{\Lambda}$ are prepared to be in the Bell states $|\Psi^{\pm}\rangle$. The additional two ancilla qubits are initialized to be in $|0\rangle$. $U_{\hat{\boldsymbol{z}}}$ and $\bar{U}_{\hat{\boldsymbol{z}}}$ are the unitary gates in which the measurement operators $M_{\hat{\boldsymbol{z}}}$ and $\bar{M}_{\hat{\boldsymbol{z}}}$ are embedded. $U(\mathcal{R})$ and $U(\bar{\mathcal{R}})$ are $SU(2)$ rotation gates. The measurements are performed on two ancilla qubits by which the quantum information in $\Lambda\bar{\Lambda}$ can be extracted.

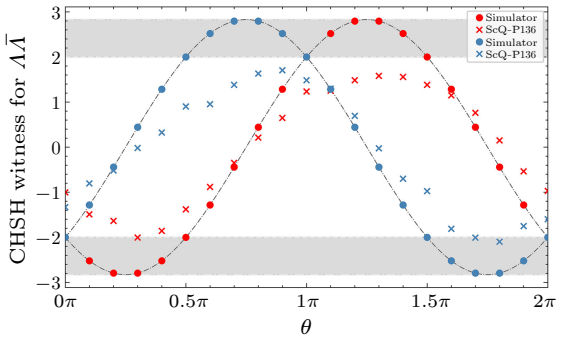

Fig. 2. The CHSH witness in the simulation of the entangled states of $\Lambda\bar{\Lambda}$. Solid circles are the results on noiseless simulator while cross symbols are the results on the superconducting quantum computer with 136 qubits. The red/blue symbols represent the initial entangled states $|\Psi^-\rangle/|\Psi^+\rangle$ for $\Lambda\bar{\Lambda}$. The shadow area is the quantum region $[-2\sqrt{2},\,-2)\cup(+2+2\sqrt{2}]$.

The simulation has been performed on simulators and the superconducting quantum computer *Quafu* developed in Beijing Academy of Quantum Information Sciences. The simulation results are shown in Fig. 2, which agree with the theoretical expectation that they enter the quantum region $[-2\sqrt{2},\,-2)\cup(2,\,2\sqrt{2}]$ and reach the maximum $2\sqrt{2}$. Thus we conclude that there is maximum violation of the CHSH inequality in $\Lambda\bar{\Lambda}$ from charmonium decays, which coincides with the result in Section 4. However, the violation of the CHSH inequality on real quantum computers turns out to be very weak. This is due to the noise in the real platform, which decreases the quantumness between two qubits. The details of our quantum simulation are shown in the Supplementary Material.

5.2 Simulation for Depolarizing Channel. As discussed in Eq. (16), the average spin density matrix of the daughter baryon in $B\to B'M$ is $\overline{\rho}_{B'}=\mathcal{E}(\rho_B)$. In the viewpoint of QIS, the post-measurement ensemble can be interpreted as a quantum evolution characterized by the quantum channel. We notice that Eq. (16) can be regarded as a single-qubit depolarizing channel as

$$\rho_B\mapsto\rho_{B'}\equiv\mathcal{E}(\rho_B)=\mathscr{P}\frac{\mathbb{1}}{2}+(1-\mathscr{P})\rho_B,\tag{32}$$

where $\mathscr{P}\equiv(2-2\gamma_B)/3$. We have a similar form for antibaryon: $\rho_{\bar{B}'}\equiv\bar{\mathcal{E}}(\rho_{\bar{B}})$ with $\bar{\mathscr{P}}\equiv(2-2\gamma_{\bar{B}})/3$. Then the average spin density matrix for $B'\bar{B}'$ from the joint decay of $B\bar{B}\to B'M\bar{B}'\bar{M}$ can be expressed as

$$\begin{aligned}\rho_{B'\bar{B}'}&=\mathcal{E}\otimes\bar{\mathcal{E}}(\rho_{B\bar{B}})\\&=\frac{1}{4}\Big[\mathbb{1}+(1-\mathscr{P})\boldsymbol{\sigma}\cdot\boldsymbol{s}_B\otimes\mathbb{1}+(1-\bar{\mathscr{P}})\mathbb{1}\otimes\boldsymbol{\sigma}\cdot\boldsymbol{s}_{\bar{B}}\\&\quad+(1-\mathscr{P})(1-\bar{\mathscr{P}})\sum_{i,j}C_{ij}\sigma_i\otimes\sigma_j\Big].\end{aligned}\tag{33}$$

Since the decay processes of B and $\bar{B}$ are not correlated, the two-qubit channel can be described as a tensor product of two independent single-qubit depolarizing channels $\mathcal{E}\otimes\bar{\mathcal{E}}$. From Eq. (33), the polarization vectors decrease by factors $(1-\mathscr{P})$ and $(1-\bar{\mathscr{P}})$, while the spin correlation decreases by a factor $(1-\mathscr{P})(1-\bar{\mathscr{P}})$. This means that the spin correlation is suppressed in decay processes. The suppression of the spin correlation may lead to the satisfaction of the CHSH inequality, since the maximal violation also decreases by the factor $(1-\mathscr{P})(1-\bar{\mathscr{P}})$, which has been discussed in Ref. [14].

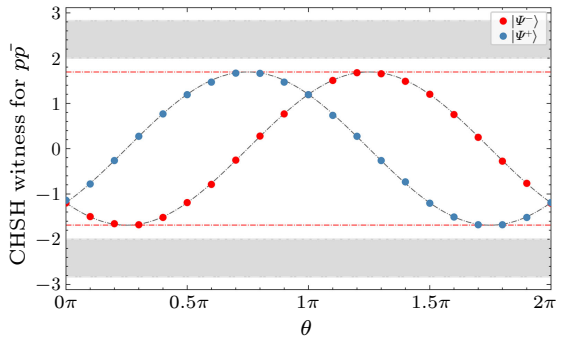

Fig. 3. The simulation results for $p\bar{p}$ in the decay $\eta_c/\chi_{c0}\to\Lambda\bar{\Lambda}\to p\pi^-\bar{p}\pi^+$ and test of the CHSH inequality. The solid circles denote the results on the noiseless simulator. The red/blue symbols represent $p\bar{p}$ produced in the subsequent decay of $\Lambda\bar{\Lambda}$ in prepared initial states $|\Psi^-\rangle/|\Psi^+\rangle$. The shadow area is the quantum region of $[-2\sqrt{2},\,-2)\cup(+2+2\sqrt{2}]$, and the red dash-dotted lines indicate the bound in Eq. (34).

We now perform a simulation based on decays $\eta_c/\chi_{c0}\to\Lambda\bar{\Lambda}\to p\pi^-\bar{p}\pi^+$. The simulation results for the channel $\rho_{p\bar{p}}=\mathcal{E}\otimes\bar{\mathcal{E}}(\rho_{\Lambda\bar{\Lambda}})$ are presented in Fig. 3. In principle, the maximum value of the Bell operator in $p\bar{p}$ becomes

$$\langle\mathcal{B}_{\mathrm{CHSH}}\rangle_{\max}=\Big(\frac{1+2\gamma_\Lambda}{3}\Big)^2 2\sqrt{2},\tag{34}$$

with $\gamma_\Lambda=\gamma_{\bar{\Lambda}}$. The data for Λ hyperon gives $\gamma_\Lambda\approx0.66$ in the Particle Data Group.[34] Thus, the maximum value is $\langle\mathcal{B}_{\mathrm{CHSH}}\rangle_{\max}\approx1.69<2$, which means that the spin correlation of $p\bar{p}$ cannot not reach the quantum bound and does not show the property of nonlocality.

In Fig. 3, we can observe that the simulation results are in agreement with our theoretical expectation that the spin correlation in decay daughters decreases in decay processes.

6. Projective Measurement and Unitary Evolution. In this section, we discuss the origin of generalized measure-

ment and its connection with particle decay/scattering processes.

In the hyperon decay $B \to B'M$, since M is a pseudoscalar meson, we can neglect its quantum state. The quantum state of the mother hyperon is $|B\rangle = |\text{momentum}\rangle \otimes |\text{spin}\rangle$ in the Hilbert space $\mathscr{H}_{\text{momentum}} \otimes \mathscr{H}_{\text{spin}}$. The general decay process can be described by a unitary evolution U called the scattering matrix S in quantum field theory. In the decay, the outgoing daughter baryon is detected in the direction $\boldsymbol{n}(\theta, \phi)$ with the angular distribution in experiments.

From the perspective of QIS, the decay process can be described as a unitary evolution governed by the Hamiltonian (or Lagrangian) of the system, $U(\rho_{\text{momentum}} \otimes \rho_{\text{spin}})U^\dagger$. Then the decay takes place by an emission of daughter particles in a certain direction, which indicates that a projective measurement is performed on the evolved system as $\Pi_{\theta\phi}U(\rho_{\text{momentum}} \otimes \rho_{\text{spin}})U^\dagger\Pi_{\theta\phi}^\dagger$, where the measurement operators are defined as projectors $\Pi_{\theta\phi} = |\theta\phi\rangle\langle\theta\phi| \in \mathscr{H}_{\text{momentum}}$. Here the quantum state of the daughter baryon $\rho_{B'} = U(\rho_{\text{momentum}} \otimes \rho_{\text{spin}})U^\dagger$ has been projected into the direction $\boldsymbol{n}(\theta, \phi)$ in momentum space. Note that the momentum magnitude $|\boldsymbol{p}|$ is fixed by the energy-momentum conservation in the two-body decay.

According to the quantum measurement postulate discussed in Section 2, the probability for finding the daughter baryon in the $\boldsymbol{n}$ direction reads

$$\mathcal{P}(\boldsymbol{n}) \propto \text{Tr}(\Pi_{\theta\phi}U(\rho_{\text{momentum}} \otimes \rho_{\text{spin}})U^\dagger\Pi_{\theta\phi}^\dagger), \tag{35}$$

where $\mathcal{P}(\boldsymbol{n})$ is just the angular distribution $(1/\Gamma)(d\Gamma/d\Omega)$. In decay or scattering processes, the momenta of initial particles are pre-determined. In the decay process, the initial momentum state is denoted as $|\mathbf{0}\rangle = |\boldsymbol{p} = \mathbf{0}\rangle$ by choosing the rest frame of mother particle, hence we have $\rho^B_{\text{momentum}} = |\mathbf{0}\rangle\langle\mathbf{0}|$ in Eq. (35). Since the initial momentum state is fixed, and the density matrix only contains the spin degree of freedom for the daughter baryon and can be obtained by taking the partial trace over momentum

$$\rho^{B'}_{\text{spin}}(\boldsymbol{n}) \propto \text{Tr}_{\text{momentum}}(\Pi_{\theta\phi}U|\mathbf{0}\rangle\rho^B_{\text{spin}}\langle\mathbf{0}|U^\dagger\Pi_{\theta\phi}^\dagger), \tag{36}$$

where the action $\text{Tr}_{\text{momentum}}$ discards the momentum degree of freedom. Considering Eqs. (2) and (14), it can be shown that $\rho^{B'}_{\text{spin}}(\boldsymbol{n}) \propto M_{\boldsymbol{n}}\rho^B_{\text{spin}}M_{\boldsymbol{n}}^\dagger$, where $\{M_{\boldsymbol{n}}\}$ denotes the generalized measurement operators induced by the partial trace over momentum.

A heuristic quantum circuit in demonstrating the decay $B \to B'M$ is shown in Fig. 4.

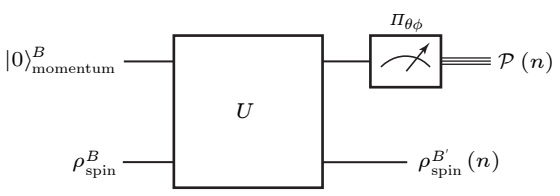

Fig. 4. A heuristic quantum circuit for demonstrating the decay $B \to B'M$.

This quantum circuit gives a pedagogical illustration of the projective measurement and unitary evolution in particle decay and scattering processes in accordance with Eqs. (35) and (36). The upper wire denotes the momentum state of the mother baryon $|\boldsymbol{p}\rangle$, which is initialized as $|\mathbf{0}\rangle$ in the rest frame, while the lower one denotes the spin state. The unitary gate U represents the unitary S-matrix in scattering theory. After the unitary evolution, a projective measurement $\Pi_{\theta\phi}$ is performed on the momentum state, resulting in the angular distribution of the daughter baryon. Consequently, the spin density operator $\rho^{B'}_{\text{spin}}(\boldsymbol{n})$ in Eq. (36) is then obtained after the projective measurement.

In quantum information theory, a unitary evolution combined with projective measurements suffices to induce a set of generalized measurements $\{M_{\boldsymbol{n}}\}$, which contain both the dynamical and measurement information of the system. The generalized measurement formalism is very useful to describe decay and scattering processes in particle physics. For more details of the topic, one can see chapter 2.2.8 of Ref. [33].

7. Summary. The particle decay processes is described as the generalized quantum measurement in quantum information theory. We consider a spin-1/2 hyperon decaying to one spin-1/2 baryon and one spin-0 meson. In this perspective, we successfully establish a correspondence between the angular distribution of the daughter baryon and the generalized measurement operator. The Bloch–Fano representation is employed to describe the quantum measurement process, which shows a direct parallelism with the decay matrices outlined in Ref. [17]. We apply this method to the joint decay of $\eta_c/\chi_{c0} \to \Lambda\bar{\Lambda} \to p\pi^+\bar{p}\pi^-$ and investigate the spin correlation in $\Lambda\bar{\Lambda}$ as well as in $p\bar{p}$ systems. The quantum simulation to test the CHSH inequality on both the simulator and real quantum computer has been carried out. A discussion on the connection between the particle decay and the generalized quantum measurement has been given.

The generalized measurement description can be applied to a wide range of decay and scattering processes. In particular, it offers us a QIS-based tool to analyze unknown particle decays in search for new physics, such as dark matter particles. It also opens a window for testing quantum nonlocality or other quantum properties in particle decays on quantum computers. Our results can be verified in particle experiments such as BESIII.[9]

Acknowledgements. We would like to thank S. Lin, D. E. Liu and R. Venugopalan for helpful discussions. We thank H.-Z. Xu for *Quafu* software and hardware supports. This work was supported by the National Natural Science Foundation of China (Grant Nos. 12135011 and 12305010), and the Strategic Priority Research Program of the Chinese Academy of Sciences (Grant No. XDB34030102).

References

[1] Afik Y and de Nova J R M 2022 *Quantum* **6** 820

[2] Altomonte C and Barr A J 2023 *Phys. Lett. B* **847** 138303
[3] Bell J S 1964 *Physics Physique Fizika* **1** 195
[4] Clauser J F and Horne M A 1974 *Phys. Rev. D* **10** 526
[5] Aspect A, Grangier P, and Roger G 1981 *Phys. Rev. Lett.* **47** 460
[6] Yin J, Cao Y, Li Y H, Liao S K, Zhang L, Ren J G, Cai W Q, Liu W Y, Li B, Dai H *et al.* 2017 *Science* **356** 1140
[7] The BIG Bell Test Collaboration 2018 *Nature* **557** 212
[8] Aspect A 2002 *Quantum Unspeakables: From Bell to Quantum Information* (Berlin: Springer) p 119
[9] The BESIII Collaboration 2019 *Nature Physics* **15** 631
[10] Törnqvist N A 1981 *Found. Phys.* **11** 171
[11] Baranov S P 2008 *J. Phys. G* **35** 075002
[12] Chen S, Nakaguchi Y, and Komamiya S 2013 *Prog. Theor. Exp. Phys.* **2013** 063A01
[13] Shi Y and Yang J C 2020 *Eur. Phys. J. C* **80** 116
[14] Qian C, Li J L, Khan A S, and Qiao C F 2020 *Phys. Rev. D* **101** 116004
[15] Khan A S, Li J L, and Qiao C F 2020 *Phys. Rev. D* **101** 096016
[16] Perotti E, Fäldt G, Kupsc A, Leupold S, and Song J J 2019 *Phys. Rev. D* **99** 056008
[17] Batozskaya V, Kupsc A, Salone N, and Wiechnik J 2023 *Phys. Rev. D* **108** 016011
[18] Gong W, Parida G, Tu Z, and Venugopalan R 2022 *Phys. Rev. D* **106** L031501
[19] Aoude R, Madge E, Maltoni F, and Mantani L 2022 *Phys. Rev. D* **106** 055007
[20] Afik Y and de Nova J R M 2023 *Phys. Rev. Lett.* **130** 221801
[21] Fabbrichesi M, Floreanini R, and Panizzo G 2021 *Phys. Rev. Lett.* **127** 161801
[22] Afik Y and de Nova J R M 2021 *Eur. Phys. J. Plus* **136** 907
[23] Fabbrichesi M, Floreanini R, and Gabrielli E 2023 *Eur. Phys. J. C* **83** 162
[24] Ehatäht K, Fabbrichesi M, Marzola L, and Veelken C 2024 *Phys. Rev. D* **109** 032005
[25] Barr A J 2022 *Phys. Lett. B* **825** 136866
[26] Barr A J, Caban P, and Rembieliński J 2023 *Quantum* **7** 1070
[27] Fabbrichesi M, Floreanini R, Gabrielli E, and Marzola L 2023 *Eur. Phys. J. C* **83** 823
[28] Ashby-Pickering R, Barr A J, and Wierzchucka A 2023 *J. High Energy Phys.* **2023** 20
[29] Barata J, Gong W J, and Venugopalan R 2024 *Phys. Rev. D* **109** 116003
[30] Pang L G, Petersen H, Wang Q, and Wang X N 2016 *Phys. Rev. Lett.* **117** 192301
[31] Lv J P, Yu Z H, Liang Z T, Wang Q, and Wang X N 2024 *Phys. Rev. D* **109** 114003
[32] Hao X Q, Ke H W, Ding Y B, Shen P N, and Li X Q 2010 *Chin. Phys. C* **34** 311
[33] Nielsen M A and Chuang I L 2015 *Quantum Computation and Quantum Information* (Cambridge: Cambridge University Press)
[34] Particle Data Group 2020 *Prog. Theor. Exp. Phys.* **2020** 083C01
[35] Lee T D and Yang C N 1957 *Phys. Rev.* **108** 1645
[36] Cronin J W and Overseth O E 1963 *Phys. Rev.* **129** 1795
[37] Baumgart M and Tweedie B 2013 *J. High Ener. Phys.* **2013** 117
[38] Horodecki R, Horodecki P, and Horodecki M 1995 *Phys. Lett. A* **200** 340